



Published in final edited form as:

J Magn Reson Imaging. 2019 March ; 49(3): 719–730. doi:10.1002/jmri.26250.

3D MR Elastography of Hepatocellular Carcinomas as a Potential Biomarker for Predicting Tumor Recurrence

Jin Wang, MD^{1,*}, Qungang Shan, MS¹, Yong Liu, MS², Hao Yang, MS¹, Sichi Kuang, MS¹, Bingjun He, BS¹, Yao Zhang, MS¹, Jingbiao Chen, MS¹, Tianhui Zhang, MS¹, Kevin J. Glaser, PhD³, Cairong Zhu, PhD⁴, Jun Chen, PhD³, Meng Yin, PhD³, Sudhakar K. Venkatesh, MD³, Richard L. Ehman, MD³

¹Department of Radiology, Sun Yat-Sen University (SYSU), Guangzhou, Guangdong, P.R. China;

²Department of Pathology, Third Affiliated Hospital, Sun Yat-Sen University (SYSU), Guangzhou, Guangdong, P.R. China;

³Department of Radiology, Mayo Clinic College of Medicine, Mayo Clinic, Rochester, Minnesota, USA;

⁴Department of Epidemiology and Biostatistics, West China School of Public Health Sichuan University, Chengdu, P.R. China

Abstract

Background: Preoperative prediction of tumor recurrence is important in the management of patients with hepatocellular carcinoma (HCC).

Purpose: To investigate whether tumor stiffness derived by magnetic resonance elastography (MRE) could predict early recurrence of HCC after hepatic resection.

Study Type: Retrospective.

Population: In all, 99 patients with pathologically confirmed HCCs after surgical resection.

Field Strength/Sequence: 3.0T; preoperative MRE with 60-Hz mechanical vibrations using an active acoustic driver.

Assessment: Regions of interest (ROIs) were manually drawn in the tumors to measure mean tumor stiffness. Surgical specimens were reviewed for histological grade, capsule, vascular invasion, and surgical margins. The early recurrence of HCC was defined as that occurring within 2 years after resection.

Statistical Tests: Cox proportional hazard models were used to evaluate risk factors associated with the time to early recurrence.

Results: HCCs with recurrence had higher tumor stiffness, higher rate of advanced T stage, vascular invasion, lower rate of capsule formation, larger tumor size, higher aspartate

*Address reprint requests to: J.W., Department of Radiology, Third Affiliated Hospital of Sun Yat-Sen University, 600 Tianhe Rd, Guangzhou 510630, People's Republic of China. wangjin3@mail.sysu.edu.cn.

Conflict of Interest

The authors report no conflicts of interest.

aminotransferase (AST), and hepatitis B virus (HBV)-DNA level and aspartate aminotransferase / alanine aminotransferase ratio ($P= 0.031, 0.007, 0.01, <0.001, 0.015, 0.034, 0.01, \text{ and } 0.014$, respectively) than HCCs without recurrence. Vascular invasion (hazard ratio [HR] = 2.922; 95% confidence interval [CI]:[1.079, 7.914], $P= 0.035$) and mean tumor stiffness (HR = 1.163; 95% CI: [1.055, 1.282], $P= 0.002$) were risk factors associated with early recurrence. Each 1-kPa increase in tumor stiffness was associated with a 16.3% increase in the risk for tumor recurrence.

Data Conclusion: The mean stiffness of HCCs may be a useful, noninvasive, quantitative biomarker for the prediction of early HCC recurrence after hepatic resection.

Level of Evidence: 4

Technical Efficacy: Stage 5

Hepatocellular carcinoma (Hcc) is the most common primary hepatic malignancy and one of the leading causes of cancer-related deaths worldwide.¹ Surgical resection, when possible, is considered to be the most effective treatment. However, patient outcomes following surgical resection are less than optimal due to tumor recurrence in approximately 50% of cases after 2 years and 75% of cases after 5 years.² Previously, tumor size, higher histological grade, vascular invasion, tumor capsule formation, and number of lesions were found to be predictive of HCC aggressiveness and recurrence after surgery. However, histological features can only be obtained after surgery.³ Therefore, identifying predictive, preoperative imaging features is crucial for the management of HCC patients awaiting surgical resection and predicting tumor recurrence after surgery.

HCC is a highly aggressive cancer with the activation of multiple signal transduction pathways, various gene mutations, and diverse etiologies that make the mechanism of HCC invasion and metastasis complex. It is reported that increased tumor stiffness promotes tumor invasion and metastasis.⁴ There are several factors that may contribute to an overall increase in tumor stiffness, including an increased extracellular matrix (ECM) stiffness secondary to collagen deposition and/or cross-linkage, abnormal perfusion, altered vasculature, and higher interstitial fluid pressure.⁵ The ECM, in particular, plays an important role in the growth of tumors and their overall structural characteristics and is related to proliferation, chemotherapeutic response, and tumor cell differentiation.⁶ Increased ECM rigidity has been shown to promote HCC progression.⁶ Increased interstitial fluid pressure is an additional contributing factor to increased tumor stiffness and is closely associated with the invasiveness and metastasis of HCC.⁷ Several staging systems based on tumor morphological characteristics and hepatic function are used by surgeons for the prediction of prognosis and the selection of treatments according to the stage.⁸

Currently, tumor characteristics mainly rely on imaging modalities such as computed tomography (CT) and magnetic resonance imaging (MRI). Hepatobiliary contrast-enhanced imaging and diffusion-weighted imaging have shown promise in evaluating the aggressiveness of HCCs, but are limited in assessing the malignant phenotype of the tumor, and this may be one of the reasons why patients of the same stage may show a different prognosis.⁹ In MRI, hypointense hepatic nodules during the hepatobiliary phase were associated with recurrence.¹⁰ CT features and the relative signal intensity of HCC in the hepatobiliary phase are also affected by liver parenchymal features that can confound

results.¹¹ A combination of morphologic features could provide a specificity >90%, but with a low sensitivity of 19.0%.¹² Low apparent diffusion coefficient (ADC) may predict recurrence of HCC after hepatectomy, but ADC measurement has poor reproducibility.¹³ The high standard uptake value in HCC using fluorodeoxyglucose positron emission tomography (FDG-PET) may be a predictor of poor prognosis in patients with HCC.¹⁴ However, it has limited sensitivity for the detection of some HCCs due to variable FDG uptake and high background liver metabolic activity.¹⁵ To overcome the above limitations, imaging modalities measuring tissue stiffness have been used to evaluate HCC characteristics and prognosis. Increased matrix stiffness promotes the progression of heat-treated residual HCC cells, proposing a new mechanism of an altered biomechanical environment following thermal ablation that accelerates HCC development.¹⁶ MR elastography (MRE) is a noninvasive method for measuring tissue stiffness. MRE-measured stiffness is useful for the staging of chronic liver disease, distinguishing malignant liver tumors from benign tumors, and predicting posthepatectomy liver failure.¹⁷⁻¹⁹ A preliminary study has shown that MRE may be able to differentiate HCC tumor grades²⁰ and provide motivation for the further evaluation of tumor stiffness in the clinical management of HCC, especially for predicting recurrence.

Chronic hepatitis B virus (HBV) accounts for more than two-thirds of HCCs in Asian countries. HBV-associated HCCs are seen in younger patients, predominantly male, and have better liver functional reserve at the time of diagnosis but present at a more advanced stage compared with hepatitis C virus (HCV)-associated HCC. However, the overall survival rate is higher in HBV-associated HCC compared with HCV-associated HCC and this is likely due to better liver parenchymal reserve and less severe hepatic inflammation.²¹⁻²³

We hypothesized that HCC stiffness evaluated with 3D MRE may be useful for predicting early recurrence of HCC after surgery. The aim of this retrospective study was to evaluate the potential utility of tumor stiffness for predicting the early recurrence of HCC following hepatic resection in patients with HBV infection.

Materials and Methods

Study Subjects

This retrospective study was approved by our Institutional Review Board and the requirement for informed consent was waived. The final study cohort consisted of 99 patients with 145 HCCs that were obtained from a historical cohort of 309 consecutive patients who had liver MRE examinations and pathologically confirmed HCCs performed at our center between December 2014 and October 2017 (Fig. 1). The 99 patients included 90 males and 9 females (mean age \pm standard deviation [SD]: 49.79 ± 11.39 years, range: 22–74 years). All patients underwent preoperative MRE, surgical resection within 1 month of the MRE examination, and regular follow-up after surgery. The mean time between MR imaging and surgery was 6.8 days (median: 6 days, range: 1–30 days). The diagnosis of HCC before surgery was based on typical hallmark imaging features according to guidelines by the American Association for the Study of Liver Diseases (AASLD).²⁴ For patients with multiple tumors, the tumor with the largest diameter in the axial imaging plane was analyzed. The surgical procedures included wedge resection ($n = 19$), segmentectomy ($n =$

25), left-lateral sectionectomy ($n = 9$), right-anterior sectionectomy ($n = 4$), right-posterior sectionectomy ($n = 7$), central hepatectomy ($n = 3$), and hemihepatectomy ($n = 32$).

Outcome

The primary outcome for this study was the early recurrence of HCC after surgical resection. Early recurrence was defined as recurrence within 2 years after curative resection of the HCC. Tumors occurring within 2 years of surgery are more likely to show the same clonal origins as the original tumor, suggesting that they had their metastatic origin shortly after the operation.²⁵ The follow-up time was calculated as the interval between resection and the date of tumor recurrence diagnosis, or as the time between the resection and the last visit if recurrence was not diagnosed.

Postoperative follow-up included clinical examination, chest radiography, biochemical liver function tests, serum levels of serum α -fetoprotein (AFP), and mean serum hepatitis B virus-DNA levels performed 1 month after hepatic resection and then every 2–3 months. In addition, contrast-enhanced ultrasound, multiphasic abdominal CT, or MRI was performed every 3 months. Increasing tumor marker levels alone without radiographic evidence of a new lesion did not indicate HCC recurrence until it was detected on imaging studies. Mean and median follow-up periods for surviving patients after hepatic resection were 7.97 and 5.39 months, respectively (range: 1.18–30.85 months). Postoperative HCC recurrence was indicated as intrahepatic recurrence, and it was considered to be present only if a newly appearing focal nodule showed hyperenhancement on arterial-phase images and washout on portal venous or delayed-phase images from dynamic CT or MRI, or by pathologic examination of resected specimens when patients underwent rehepatectomy.²⁶

Laboratory Assessment

Subjects underwent standardized evaluation of clinical history, physical and anthropometric exams, and laboratory tests within 2 weeks of MRE. Several blood test indices including aspartate aminotransferase (AST), alanine aminotransferase (ALT), AST/ALT ratio, total bilirubin, albumin, prothrombin time, AFP, mean serum HBVDNA levels, hemoglobin, white blood cells, sodium, creatinine, neutrophil-to-lymphocyte ratio, and platelet count were recorded by referring to previous studies.²⁵

Pathology Review

Histology specimens were obtained from surgical resection in all patients. An experienced hepatopathologist (21 years of experience) blinded to all clinical data and MRE results reviewed the hematoxylin-and-eosin-stained slides for capsule formation, histological grade, vascular invasion, and clean surgical margins according to the World Health Organization classification system.^{27,28} All pathologic parameters were considered as categorical variables: histological grade (well/moderately/poorly differentiated), vascular invasion (no invasion/microvascular invasion/macrovascular invasion) and tumor capsule formation (absent/present). Microvascular invasion was defined as seen only on microscopy, and macrovascular invasion was defined as visible on radiological imaging or on gross examination. When different grades coexisted within a tumor, the predominant grade of the tumor was used (>50%). Tumor capsule formation was considered positive when the capsule

was found along at least two-thirds of the tumor margin, regardless of the presence of microscopic capsular or extracapsular invasion.²⁹ The surgical margin of the tumor was assessed to confirm if it was clear. The liver fibrosis stage of the nontumor-bearing liver parenchyma was assessed from the resected specimens using the METAVIR staging system.³⁰ Based on the prognostic significance, tumor size was categorized as <5 cm and ≥5 cm.

MRE

All subjects underwent conventional MRI and MRE examinations using a 3.0T MR system (Discovery MR750, GE Healthcare, Milwaukee, WI) with an 8-channel, phased-array, torso coil. To reduce potential physiological confounding factors, patients were instructed to fast for a minimum of 4 hours before the MRE exams. 3D liver MRE was performed before any intravenous contrast was given, as previously described, using a multislice, flow-compensated, spin-echo echo-planar imaging (SE-EPI), MRE sequence.¹⁹ A pneumatic, passive, drum driver was placed, over the left or right tumor-containing lobe of the liver, at the level of the xiphisternum and was secured with an elastic belt. Continuous, 60-Hz, mechanical vibrations were generated using an active acoustic driver located outside of the scan room and were transmitted through polyvinyl chloride tubing to the passive driver to produce shear waves in the liver.³ The total imaging time for MRE was about 64 seconds, performed in either three 21-second breath-holds or six 11-second breath-holds. The MRE parameters included: acquisition matrix = 80 × 80; repetition time = 1334 msec; echo time = 52 msec; one EPI shot; field of view = 44.8 cm; number of slices = 32; slice thickness = 3.6 mm, inter-slice gap = 0 mm, superior–inferior spatial saturation bands, and parallel imaging acceleration factor = 2. The MRE phase images were processed using a 3D direct inversion of the Helmholtz wave equations using the curl of the measured wave field to generate images of the stiffness distribution in the liver and tumors (elastograms).³¹

Image Analysis and Tumor Stiffness Measurement

MRE images were interpreted in consensus by a board-certified abdominal radiologist with 24 years of experience and one experienced engineer with 18 years of MRE experience to assess image quality and the reliability of the tumor stiffness measurements.¹⁹ The diagnosis of HCC was based on the noninvasive criteria proposed by the AASLD recommendations, including washin in the arterial phase and washout in the portal or delayed phase.²⁴ Tumor stiffness was measured independently by a radiologist with 5 years of experience in liver MRI who was blinded to all clinical and tumor pathology data. For the purpose of assessing the reliability of the measurements of tumor stiffness, 60 (60.6%) patients were randomly selected for repeated, blinded measurements performed independently by another radiologist with 6 years of experience.

The tumor stiffness was considered reliable when an interquartile range (IQR)/median value was less than 0.30.³² Regions of interest (ROIs) were manually drawn tracing the HCC on every slice demonstrating the tumor and covering the entire tumor on the magnitude images using T₂-weighted and contrast-enhanced images as references. The mean liver stiffness, in kPa, and the ROI area were recorded. The ROIs were drawn as large as possible while excluding tumor edges (where partial-volume effects likely affected the calculated stiffness)^{19,33,34}; areas of significant wave interference (such as liquefactive necrosis in the

tumor), and any other artifacts seen on the magnitude and phase images. Whole-tumor volume was automatically calculated by multiplying the cross-sectional area by the section thickness (ie, the sum of the area in all ROIs drawn times the section thickness) using a manufacturer-developed tool. This was done to reflect the histology and characteristics of the tumor more accurately. The mean stiffness from the ROIs and the ROI area for each tumor were recorded. Separate ROIs were drawn on the liver parenchyma around the tumor (avoiding regions with significant wave interference, large vessels, and bile ducts) and the mean stiffness was obtained by pooling the ROIs drawn on all sections.³³

Statistical Analyses

Data for continuous measures are summarized as mean \pm SD when the *t*-test was used, but as the median (IQR) when the Mann–Whitney test was used. Categorical variables were analyzed using a chi-square test or Fisher’s exact test.

Interobserver agreement of the tumor stiffness measurements on the same lesion between two radiologists was evaluated using the intraclass correlation coefficient (ICC) along with its 95% confidence interval (CI). Comparisons were made for tumor stiffness and histological results. The univariate Cox proportional hazard model was performed first to evaluate the association between time to early recurrence and each individual risk factor, such as tumor stiffness, number of tumors, tumor size, histological grade, vascular invasion, capsule, age, gender, serum AFP level, AST, AST/ALT, HBV-DNA, body mass index, liver parenchyma stiffness, and fibrosis stage. For adjusting potential confounding factors, the multivariate Cox proportional hazard model was used to identify independent risk factors for the time to early recurrence. The variables that were significant ($P < 0.100$) in the univariate analysis were included in the initial multivariate model to derive the final model. Hazard ratios (HRs) and their 95% CIs were presented. All the statistical analyses were performed using SPSS v. 22.0 (IBM, Armonk, NY). $P < 0.05$ for two-sided tests was considered statistically significant.

Results

The median body mass index was 22.02 kg/m² (IQR: 19.92–24.91 kg/m²). The median serum hepatitis B virus-DNA levels were 0.020×10^5 IU/mL (IQR: 0.00012– 1.14×10^5 IU/mL). Sixty-two patients (63%) had advanced liver fibrosis (F3-F4). Surgical margins were clear in all the resected species. No patients died during the follow-up.

The size (diameter) of the tumors ranged from 23–155 mm (median: 48 mm, IQR: 37.00–72.00 mm). Forty-eight patients had tumors with diameters ≥ 5 cm and 51 patients had tumors < 5 cm, including 12/51 patients with tumors < 3 cm. HCC with clean surgical margins was confirmed in each hepatectomy specimen. The majority of patients (72/99, 72.7%) had a single HCC. Seventy-two HCCs (72.7%) had capsules and 27 (27.3%) did not have any capsule. Tumor grade was well differentiated in 11 patients (11.1%), moderately differentiated in 73 (73.7%), and poorly differentiated in 15 (15.2%). Fifty-nine (60%) patients had vascular invasion, of which 12 had macrovascular invasion on MRI or gross examination. HCC volume ranged from 140–45,758 mm³ with a mean of 5839 mm³ (median: 1840 mm³) (Figs. 2–5). The mean HCC stiffness measured by observer 1 and

observer 2 ranged from 2.40–18.58 kPa (median: 5.26 kPa, IQR: 4.75–6.26 kPa, IQR/median: 0.29) and 2.40–18.58 kPa (median: 5.43 kPa, IQR: 4.59–6.15 kPa, IQR/median: 0.29). There was excellent interobserver reproducibility of HCC stiffness, with an ICC of 0.965 (95% CI: 0.943–0.979). The liver parenchyma stiffness ranged from 1.78–10.90 kPa (median: 2.90 kPa, IQR: 2.54–3.34 kPa). The liver parenchyma stiffness with early-stage fibrosis ranged from 1.78–4.65 kPa (median: 2.60 kPa, IQR: 2.21–2.96 kPa), and with advanced fibrosis ranged from 1.86–10.90 kPa (median: 3.08 kPa, IQR: 2.79–3.71 kPa). HCCs with capsule had significantly lower mean stiffness as compared with HCCs without capsule (4.77 (4.011–6.36) kPa vs. 7.03 (5.58–9.50) kPa, $P < 0.001$). HCCs with vascular invasion had a higher stiffness compared with those without vascular invasion (5.77 (4.35–7.32) kPa vs. 4.67 (4.04–5.98) kPa, $P = 0.018$). There was a significant difference in tumor stiffness between well and/or moderately differentiated HCCs and poorly differentiated HCCs (4.91 (4.01–6.48) kPa vs. 7.28 (5.68–9.80) kPa, $P = 0.001$).

Comparison of Patients With and Without Recurrence

Twenty-nine of the 99 patients showed early tumor recurrence within 2 years (recurrence rate of 27.3%). The demographics and clinical pathological characteristics of patients with and without recurrence are compared in Table 1. Tumor stiffness of HCCs with recurrence was significantly higher than that of HCCs without recurrence (5.89 (4.34–9.10) kPa vs. 4.87 (4.08–6.57) kPa; $P = 0.031$). HCCs with recurrence had a higher rate of advanced T stage; larger tumor size; and higher AST, HBV-DNA, and AST/ALT ratio ($P = 0.007, 0.015, 0.034, 0.01, \text{ and } 0.014$, respectively) than HCCs without recurrence. Moreover, HCCs with recurrence showed much lower incidence of capsule formation and higher incidence of vascular invasion ($P < 0.001$ and 0.01 , respectively).

Factors Associated With Early Recurrence of HCC

There was no significant correlation between liver parenchyma stiffness and recurrence ($P = 0.699$). Univariate analysis showed that tumor size (HR = 2.618, 95% CI: [1.190, 5.758], $P = 0.017$), histological grade (HR = 2.527, 95% CI: [1.093, 5.843], $P = 0.03$), vascular invasion (HR = 3.695, 95% CI: [1.402, 9.736], $P = 0.008$), capsule (HR = 3.087, 95% CI: [1.479, 6.442], $P = 0.003$), and tumor stiffness (HR = 1.203, 95% CI: [1.095, 1.321], $P < 0.001$) were associated with early recurrence. HCC size, histological grade, vascular invasion, capsule, and stiffness were included in the initial multivariate model to derive the final model. The multivariate Cox proportional hazard model showed that vascular invasion (HR = 2.922; 95% CI: [1.079, 7.914], $P = 0.035$) and tumor stiffness (HR = 1.163; 95% CI: [1.055, 1.282], $P = 0.002$) were risk factors associated with early recurrence (Table 2). Each 1-kPa increase in tumor stiffness was associated with a 16.3% increase in the risk for tumor recurrence.

There were 77 patients with a single HCC who were used for subgroup analysis. Univariate analysis showed that tumor size (HR = 3.131, 95% CI: [1.184, 8.282], $P = 0.021$), vascular invasion (HR = 4.434, 95% CI: [1.289, 15.251], $P = 0.018$), capsule (HR = 3.713, 95% CI: [1.430, 9.640], $P = 0.007$) and tumor stiffness (HR = 1.196, 95% CI: [1.055, 1.356], $P = 0.005$) were associated with early recurrence. The variables size, histological grade, vascular invasion, capsule, and stiffness were included in the initial multivariate model to derive the

final model. The multivariate Cox proportional hazard model showed that vascular invasion (HR = 3.773; 95% CI: [1.073, 13.264], $P = 0.038$) and tumor stiffness (HR = 1.150; 95% CI: [1.013, 1.307], $P = 0.031$) were risk factors associated with early recurrence (Table 3).

Discussion

The results of our study show that HCCs that were poorly differentiated, had no capsule, and had vascular invasion were significantly stiffer than well or moderately differentiated HCCs, HCCs with capsule, and HCCs without vascular invasion. High HCC stiffness was also associated with high recurrence following hepatic resection. Our study also confirmed that higher tumor stiffness, large size, advanced T-stage, vascular invasion, absence of capsule, high HBV DNA levels, higher AST levels, and a higher serum AST/ALT ratio were associated with recurrence. Multivariate analysis showed that only vascular invasion and mean HCC stiffness were risk factors associated with early recurrence. MRE may therefore be useful as a potential noninvasive imaging biomarker for predicting early recurrence.

Several imaging studies have attempted to differentiate HCCs using dynamic contrast-enhanced MRI, hepatobiliary phase (HBP) imaging, diffusion-weighted imaging, and intra-voxel incoherent motion. Morphologic features such as tumor size, nonsmooth tumor margins, and peritumoral enhancement have high accuracy in the prediction of microvascular invasion in HCCs; the sensitivity is relatively low,³⁰ HCCs may show hyper-, iso-, and hyperintensity on HBP images, and Choi et al considered that iso- to hyperintensity on HBP images may be a useful imaging biomarker to indicate prognosis after surgery.¹¹ Although ADC measurements have promise, they also have several limitations, including variable b-values, with no consensus among researchers, and other technical limitations.³¹ The absence of a tumor capsule and an indistinct margin on CT were found to predict early recurrence after surgical resection in one study,²⁹ suggesting a need for additional biomarkers to identify vascular invasion.

Although additional equipment is necessary to quantify tumor stiffness with MRE, it provides a new way to assess HCC aggressiveness. In our study, all cases showed washin/out enhancement patterns according to AASLD criteria in conventional MR, but our results showed that some tumors were stiff and others were soft. The tumor capsule is recognized as a barrier preventing the spread of cancer cells and the presence of a capsule has been considered a significant and independent predictive factor of overall survival and recurrence, even in small HCCs.³⁵ Encapsulated HCCs are associated with less vascular invasion, lower tumor stage, and smaller tumor size.^{3,5} Vascular invasion represents one of the most important prognostic factors for tumor recurrence and overall survival after HCC resection and this feature is included in major Society guidelines.³⁶ Microvascular and macrovascular invasion are associated with a 4.4-fold and 15-fold increased risk of tumor recurrence, respectively.³⁷ Poorly differentiated HCCs are associated with a higher recurrence rate (2-fold increase) and lower survival rate compared with well and moderately differentiated HCCs.³ Our results showed that HCCs that were poorly differentiated, had no capsule, and had vascular invasion were significantly stiffer than well or moderately differentiated HCCs, HCCs with capsule, and HCCs without vascular invasion, suggesting a possible role for MRE as a noninvasive indicator of these tumor characteristics. Our results also showed that

patients with recurrence tend to have vascular invasion, no capsule, and higher tumor stiffness in addition to higher serum AST/ALT, AST, and HBV-DNA levels, larger tumor size, and advanced T stage. HCCs with recurrence tended to be poorly differentiated compared with HCCs without recurrence, but this did not show a significant difference, which may be due to our small sample size.

A previous sono-elastography study reported that tumor stiffness was higher in poorly differentiated lesions than in moderately to well-differentiated lesions, which is consistent with our results.³⁸ This indicates the potential value of tumor stiffness as a noninvasive biomarker for the aggressiveness of HCCs. Our results are different from that of a recent study by Thompson et al²⁰ using 2D MRE that showed that well or moderately differentiated HCCs were stiffer than poorly differentiated HCCs. However, their study population was much smaller than ours and they used a 2D MRE technique with just four, 1-cm-thick slices, which may introduce measurement biases or variances due to the complicated, 3D nature of wave propagation in tumors. Our 3D MRE technique may have provided better estimates of stiffness that are less subject to partial volume effects and other artifacts than the 2D method.²⁰ In addition, in their study ROIs were drawn by excluding necrotic components according to enhancement, which may be subjective and lead to interobserver variability. By contrast, in our study whole tumor analysis was used and it may provide more precise information, reflect the tumor heterogeneity better, and mitigate interobserver variability. However, we did exclude from this study tumors that were less than 2 cm to avoid incorrect tumor stiffness measurements due to the low resolution of MRE, and any areas of significant wave interference due to obvious liquefactive necrosis in the tumor. The reproducibility of the HCC stiffness measurements was excellent. These may explain the discrepancy between our study and theirs. A future study with serial MRE measurements may be useful to determine if there are changes in tumor stiffness with the evolution of HCC. In this study, only HBV-related HCC patients were included. HBV infection is the main risk factor of HCC in China. In addition, larger tumor size, multiple nodules, and vascular invasion are more frequent in HBV-related HCC compared with HCC caused by other factors.^{22,23}

Since early tumor recurrence is associated with a worse prognosis, preoperative evaluation with MREs may be useful for identifying patients with a higher risk of recurrence so that alternative treatment options may be considered. MRE is a reliable method for assessing tissue stiffness, with little variability between image manufacturers, field strengths, and pulse sequences.^{19,39} Each 1-kPa increase in tumor stiffness was associated with a 16.3% increase in the risk for tumor recurrence, suggesting a possible role for MRE as a method to evaluate histological features and aggressiveness of HCCs. Tumor stiffness measured using MRE adds to the growing list of candidate imaging biomarkers for HCC.²⁰ Previous studies reported that background liver stiffness measured by MRE is an independent risk factor for the development of HCC in chronic liver disease, with cirrhotic patients having a 2.4-fold increased risk of developing a late recurrence when compared with noncirrhotic patients.⁴⁰ We did not find any such correlation in our study. This is probably due to the relatively small sample size of patients with advanced fibrosis and shorter follow-up period in our study. The recurrence rate of HCC after hepatic resection was lower in our study compared with other reports, which may be attributable to the small sample size in our study.² Future prospective studies involving a larger cohort of patients and a longer longitudinal follow-up are needed

to systematically investigate radiologic-pathologic correlates and their predictive capability for early and late recurrence in order to explore the role of tumor stiffness in the development of HCC.

There were several limitations to our study. The retrospective design of cases from a single scanner from one MRI vendor at one institution, together with the selection of surgical candidates and the small number of small HCCs, may not represent a normal or general clinical spectrum of cases and imaging results. Our cohort had 80% of patients with well or moderately differentiated HCCs. Our patients were chronic hepatitis B carriers, whereas the incidence of HBV infection is lower in Europe and Western countries, and the conclusion may not be generalizable to patients with other etiologies. It would be useful to perform a similar study in a Western population and with different chronic liver disease etiologies. This is a pilot study and the follow-up time was short. We will see if more insights can be drawn from a larger case pool in the future. Newer imaging methods, such as hepatobiliary phase imaging with liver-specific contrast agents, were not compared, as this was not the aim of the study. It is possible that liver MRE using a 60-Hz vibration frequency may be less effective in resolving small, stiff HCCs due to the long shear wavelength, and the use of higher vibration frequencies may have to be considered for smaller tumors. HCCs are inhomogeneous and the ROIs used in this study covered the whole tumor, thus mixed components, including necrosis and hemorrhage, were also included, which may have affected the assessment of the tumor stiffness. The mean tumor stiffness used in our study may not adequately reflect the heterogeneity of HCCs and some form of histogram analysis might be useful in future studies. Although the mean time between the surgery and MRI was less than 1 week, there may have been variations in the HCC and hepatic parenchyma stiffness even in that time frame. Lastly, we only analyzed the stiffness of the largest lesion in patients with multiple tumors, which may have variable intralesional components that have variable elastic values, and the largest tumor may not reflect the invasiveness of other HCCs and the aggressive behavior of smaller HCCs. We did a subanalysis to assess the early recurrence of HCCs in patients with only one tumor, and it showed vascular invasion and mean tumor stiffness were independent risk factors associated with early recurrence.

In conclusion, tumor stiffness measured by 3D MRE is a significant noninvasive risk factor associated with the early recurrence of HBV-related HCCs after hepatic resection. Each 1-kPa increase in tumor stiffness was associated with a 16.3% increase in the risk for tumor recurrence. More studies using tumor stiffness are warranted to further explore this field, which will improve our understanding of the relationship between HCC stiffness, invasiveness, and outcome for better allocation of treatment strategies and surveillance follow-up.

Acknowledgment

Contract grant sponsor: National Natural Science Foundation of China; Contract grant number: 81271562 (to J.W.); Contract grant sponsor: Science and Technology Program of Guangzhou, China; Contract grant number: 01704020016 (to J.W.); Contract grant sponsor: National Institutes of Health (NIH); Contract grant numbers: EB001981 (to R.L.E.) and EB017197 (to M.Y.) to design and conduct the study and collect, manage, and analyze the data.

References

1. Yang JD, Roberts LR. Epidemiology and management of hepatocellular carcinoma. *Infect Dis Clin North Am* 2010;24:899–919, viii. [PubMed: 20937457]
2. Maluccio M, Covey A. Recent progress in understanding, diagnosing, and treating hepatocellular carcinoma. *CA Cancer J Clin* 2012;62: 394–399. [PubMed: 23070690]
3. Colecchia A, Schiumerini R, Cucchetti A, et al. Prognostic factors for hepatocellular carcinoma recurrence. *World J Gastroenterol* 2014;20: 5935–5950. [PubMed: 24876717]
4. Wei SC, Fattet L, Tsai JH, et al. Matrix stiffness drives epithelial-mesenchymal transition and tumour metastasis through a TWIST1-G3BP2 mechanotransduction pathway. *Nat Cell Biol* 2015;17: 678–688. [PubMed: 25893917]
5. Pepin KM, Ehman RL, McGee KP. Magnetic resonance elastography (MRE) in cancer: Technique, analysis, and applications. *Prog Nucl Magn Reson Spectrosc* 2015;90–91:32–48.
6. Lu P, Weaver VM, Werb Z. The extracellular matrix: A dynamic niche in cancer progression. *J Cell Biol* 2012;196:395–406. [PubMed: 22351925]
7. Colombo J, Maciel JM, Ferreira LC, RF DAS, Zuccari DA. Effects of melatonin on HIF-1alpha and VEGF expression and on the invasive properties of hepatocarcinoma cells. *Oncol Lett* 2016;12:231–237. [PubMed: 27347130]
8. Sala M, Forner A, Varela M, Bruix J. Prognostic prediction in patients with hepatocellular carcinoma. *Semin Liver Dis* 2005;25:171–180. [PubMed: 15918146]
9. Cillo U, Giuliani T, Polacco M, Herrero Manley LM, Crivellari G, Vitale A. Prediction of hepatocellular carcinoma biological behavior in patient selection for liver transplantation. *World J Gastroenterol* 2016;22: 232–252. [PubMed: 26755873]
10. Lee DH, Lee JM, Lee JY, et al. Non-hypervascular hepatobiliary phase hypointense nodules on gadoxetic acid-enhanced MRI: Risk of HCC recurrence after radiofrequency ablation. *J Hepatol* 2015;62:1122–1130. [PubMed: 25529623]
11. Choi JW, Lee JM, Kim SJ, et al. Hepatocellular carcinoma: Imaging patterns on gadoxetic acid-enhanced MR Images and their value as an imaging biomarker. *Radiology* 2013;267:776–786. [PubMed: 23401584]
12. Lee S, Kim SH, Lee JE, Sinn DH, Park CK. Preoperative gadoxetic acid-enhanced MRI for predicting microvascular invasion in patients with single hepatocellular carcinoma. *J Hepatol* 2017;67:526–534. [PubMed: 28483680]
13. Iima M, Le Bihan D. Clinical intravoxel incoherent motion and diffusion MR imaging: Past, present, and future. *Radiology* 2016;278:13–32. [PubMed: 26690990]
14. Ahn SG, Kim SH, Jeon TJ, et al. The role of preoperative [18F]fluorodeoxyglucose positron emission tomography in predicting early recurrence after curative resection of hepatocellular carcinomas. *J Gastrointest Surg* 2011;15:2044–2052. [PubMed: 21904962]
15. Ahn SY, Lee JM, Joo I, et al. Prediction of microvascular invasion of hepatocellular carcinoma using gadoxetic acid-enhanced MR and (18) F-FDG PET/CT. *Abdom Imaging* 2015;40:843–851. [PubMed: 25253426]
16. Zhang R, Ma M, Dong G, et al. Increased matrix stiffness promotes tumor progression of residual hepatocellular carcinoma after insufficient heat treatment. *Cancer Sci* 2017;108:1778–1786. [PubMed: 28699238]
17. Lee DH, Lee JM, Yi NJ, et al. Hepatic stiffness measurement by using MR elastography: Prognostic values after hepatic resection for hepatocellular carcinoma. *Eur Radiol* 2017;27:1713–1721. [PubMed: 27456966]
18. Kennedy P, Wagner M, Castera L, et al. Quantitative elastography methods in liver disease: Current evidence and future directions. *Radiology* 2018;286:738–763. [PubMed: 29461949]
19. Wang J, Glaser KJ, Zhang T, et al. Assessment of advanced hepatic MR elastography methods for susceptibility artifact suppression in clinical patients. *J Magn Reson Imaging* 2018;47:976–987. [PubMed: 28801939]
20. Thompson SM, Wang J, Chandan VS, et al. MR elastography of hepato-cellular carcinoma: Correlation of tumor stiffness with histopathology features-Preliminary findings. *Magn Reson Imaging* 2017;37:41–45. [PubMed: 27845245]

21. de Martel C, Maucort-Boulch D, Plummer M, Franceschi S. World-wide relative contribution of hepatitis B and C viruses in hepatocellular carcinoma. *Hepatology* 2015;62:1190–1200. [PubMed: 26146815]
22. Kao WY, Su CW, Chau GY, Lui WY, Wu CW, Wu JC. A comparison of prognosis between patients with hepatitis B and C virus-related hepato-cellular carcinoma undergoing resection surgery. *World J Surg* 2011;35: 858–867. [PubMed: 21207029]
23. Zhou Y, Si X, Wu L, Su X, Li B, Zhang Z. Influence of viral hepatitis status on prognosis in patients undergoing hepatic resection for hepatocellular carcinoma: A meta-analysis of observational studies. *World J Surg Oncol* 2011;9:108. [PubMed: 21933440]
24. Bruix J, Sherman M, American Association for the Study of Liver D. Management of hepatocellular carcinoma: An update. *Hepatology* 2011;53: 1020–1022. [PubMed: 21374666]
25. Wu JC, Huang YH, Chau GY, et al. Risk factors for early and late recurrence in hepatitis B-related hepatocellular carcinoma. *J Hepatol* 2009;51: 890–897. [PubMed: 19747749]
26. Toyoda H, Kumada T, Tada T, et al. Non-hypervascular hypointense nodules detected by Gd-EOB-DTPA-enhanced MRI are a risk factor for recurrence of HCC after hepatectomy. *J Hepatol* 2013;58:1174–1180. [PubMed: 23376360]
27. Kleihues P, Sobin LH. World Health Organization classification of tumors. *Cancer* 2000;88:2887. [PubMed: 10870076]
28. Aaltonen LAH, Stanley R. Pathology and genetics of tumours of the digestive system. Lyon, Oxford: IARC Press; Oxford University Press (distributor) 2000 p 265–314.
29. Ishigami K, Yoshimitsu K, Nishihara Y, et al. Hepatocellular carcinoma with a pseudocapsule on gadolinium-enhanced MR images: Correlation with histopathologic findings. *Radiology* 2009;250:435–443. [PubMed: 19095782]
30. Bedossa P, Poynard T. An algorithm for the grading of activity in chronic hepatitis C. The METAVIR Cooperative Study Group. *Hepatology* 1996; 24:289–293. [PubMed: 8690394]
31. Loomba R, Cui J, Wolfson T, et al. Novel 3D magnetic resonance elastography for the noninvasive diagnosis of advanced fibrosis in NAFLD: A prospective study. *Am J Gastroenterol* 2016;111:986–994. [PubMed: 27002798]
32. Boursier J, Zarski JP, de Ledinghen V, et al. Determination of reliability criteria for liver stiffness evaluation by transient elastography. *Hepatology* 2013;57:1182–1191. [PubMed: 22899556]
33. Yin M, Glaser KJ, Talwalkar JA, Chen J, Manduca A, Ehman RL. Hepatic MR elastography: Clinical performance in a series of 1377 consecutive examinations. *Radiology* 2016;278:114–124. [PubMed: 26162026]
34. Wang JYH, Liu Y. Using tumor stiffness as a potential biomarker for predicting hepatocellular carcinoma recurrence. In: *Proc ISMRM*; 2018:6089.
35. Takeishi K, Maeda T, Shirabe K, et al. Clinicopathologic features and outcomes of non-B, non-C hepatocellular carcinoma after hepatectomy. *Ann Surg Oncol* 2015;22(Suppl 3):S1116–1124. [PubMed: 26159442]
36. European Association For The Study Of The L, European Organisation For R, Treatment Of C. EASL-EORTC clinical practice guidelines: Management of hepatocellular carcinoma. *J Hepatol* 2012;56:908–943. [PubMed: 22424438]
37. Miyata R, Tanimoto A, Wakabayashi G, et al. Accuracy of preoperative prediction of microinvasion of portal vein in hepatocellular carcinoma using superparamagnetic iron oxide-enhanced magnetic resonance imaging and computed tomography during hepatic angiography. *J Gastroenterol* 2006;41:987–995. [PubMed: 17096068]
38. Ling W, Lu Q, Lu C, et al. Effects of vascularity and differentiation of hepatocellular carcinoma on tumor and liver stiffness: in vivo and in vitro studies. *Ultrasound Med Biol* 2014;40:739–746. [PubMed: 24412176]
39. Chen J, Yin M, Talwalkar JA, et al. Diagnostic performance of MR elastography and vibration-controlled transient elastography in the detection of hepatic fibrosis in patients with severe to morbid obesity. *Radiology* 2017;283:418–428. [PubMed: 27861111]
40. Wu D, Chen E, Liang T, et al. Predicting the risk of postoperative liver failure and overall survival using liver and spleen stiffness measurements in patients with hepatocellular carcinoma. *Medicine (Baltimore)* 2017;96: e7864. [PubMed: 28834899]

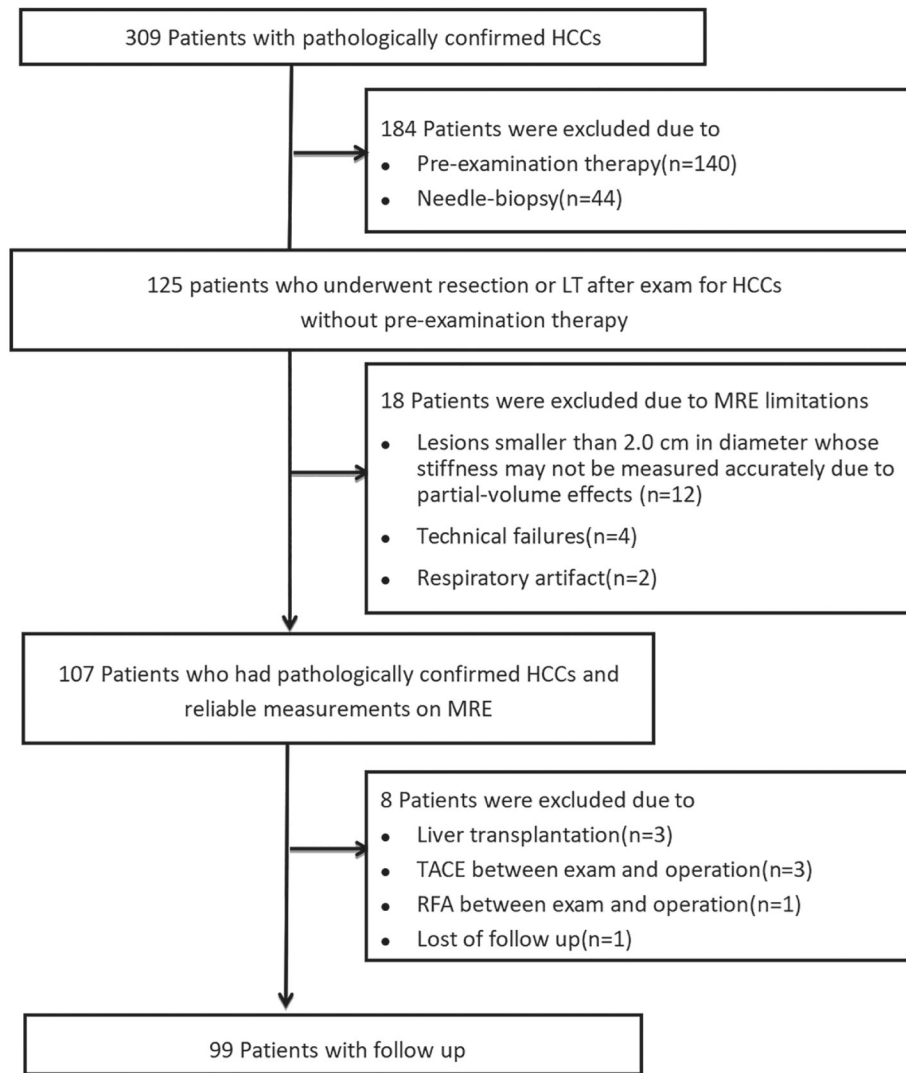


FIGURE 1:
Flowchart shows inclusion and exclusion criteria for the study.

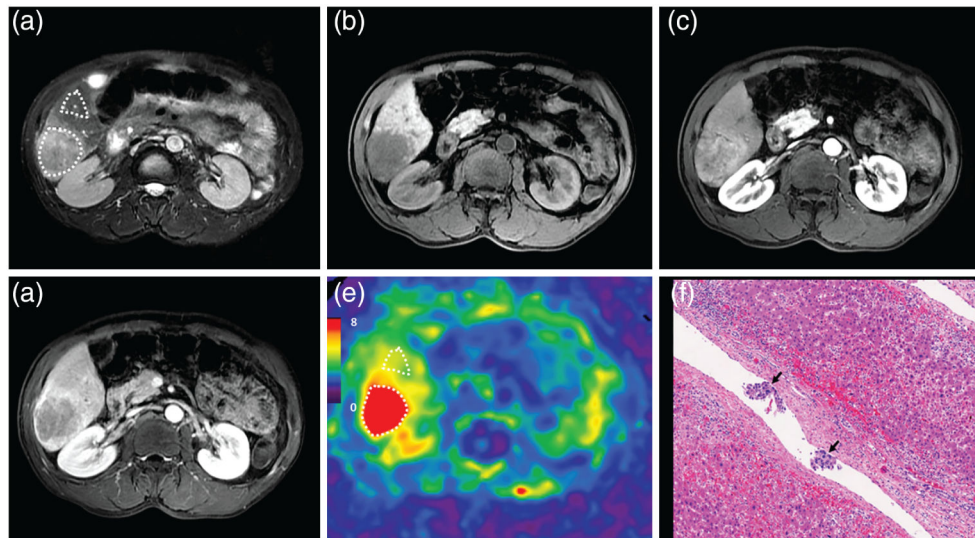


FIGURE 2:

A 55-year-old male patient with a poorly differentiated HCC without capsule formation, with vascular invasion, and without early recurrence after 9.8 months. MRI shows a mass in the right lobe of the liver with mild-moderate hyperintensity on T₂WI (a) and hypointensity on precontrast T₁WI (b). Contrast-enhanced MRI shows typical washin in the arterial phase (c) and washout in the portal venous phase (d). The 3D elastogram (e) shows that the HCC was very stiff. The mean tumor stiffness was 14.87 kPa and the mean liver parenchyma stiffness was 4.96 kPa. Photomicrograph (f) of H&E-stained ($\times 100$) shows tumor thrombus in a vessel.

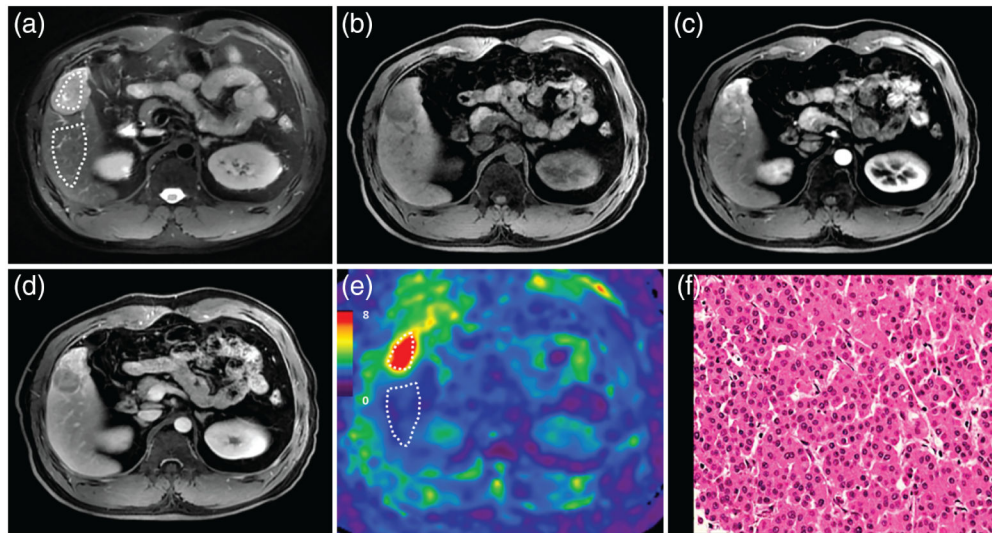
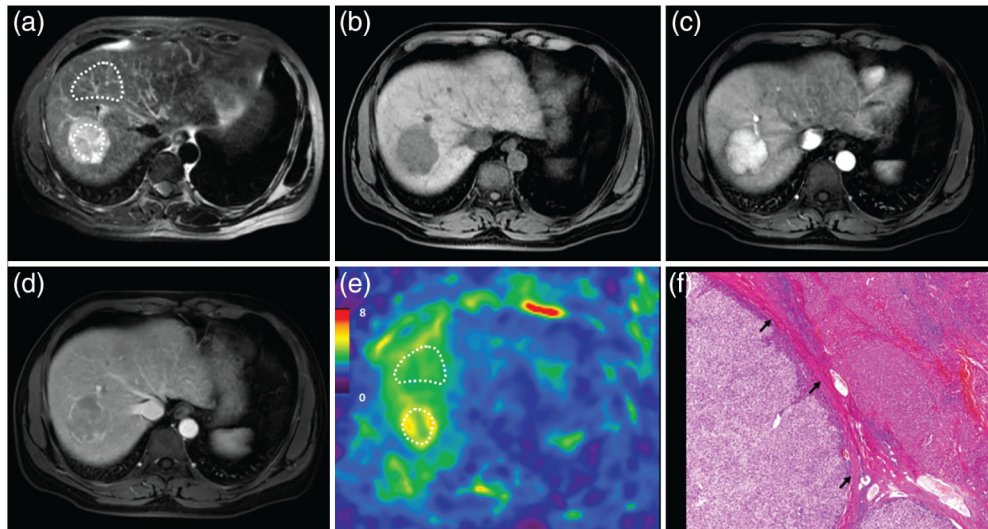


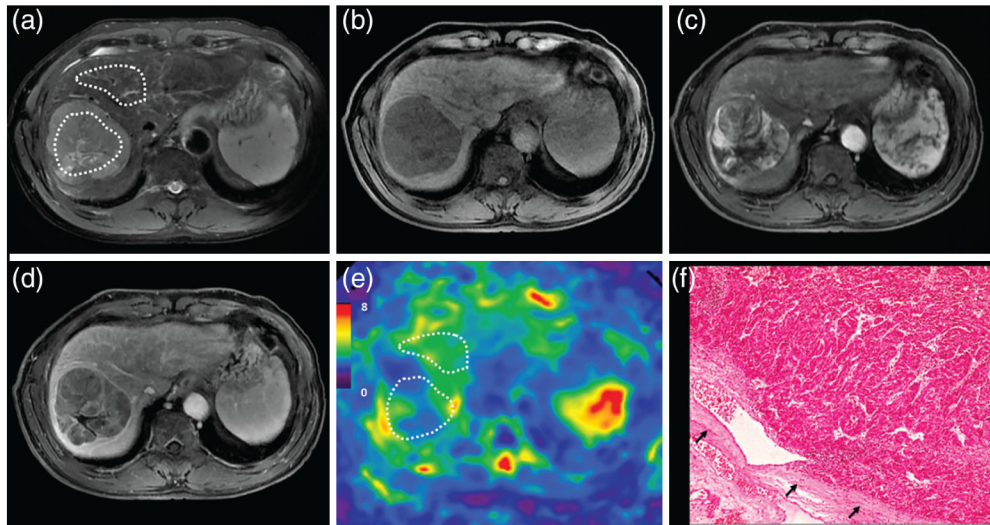
FIGURE 3:

A 37-year-old male patient with a moderately differentiated HCC with capsule, without vascular invasion, and with early recurrence after 3 months. MRI shows a mass in S5 of the liver with mild-moderate hyperintensity on T₂WI (a). The mass is hypointense on precontrast T₁WI (b) and shows typical washin in the arterial phase (c), and washout in the portal venous phase (d). The 3D elastogram (e) shows that the HCC is stiff. The mean tumor stiffness was 8.84 kPa and the mean liver parenchyma stiffness was 1.91 kPa.

Photomicrograph (f) of H&E-stained ($\times 400$) of moderately differentiated HCC shows abundant atypical hepatocytes with high cellularity.

**FIGURE 4:**

A 41-year-old male patient with a moderately differentiated HCC with capsule, without vascular invasion, and without recurrence after 11.7 months. MRI shows a mass in the right lobe of the liver with mild-moderate hyperintensity on T₂WI (a). The mass is hypointense on precontrast T₁WI (b) and shows typical wash-in in the arterial phase (c), and washout in the portal venous phase (d). The 3D elastogram (e) shows that the HCC is a little stiffer than the parenchyma. The mean tumor stiffness was 4.71 kPa and the mean liver parenchyma stiffness was 3.93 kPa. Photomicrograph (f) of H&E-stained (×20) shows tumor with peritumoral fibrosis.

**FIGURE 5:**

A 72-year-old male patient with a moderately differentiated HCC with capsule formation, without vascular invasion, and without early recurrence after 15.7 months. MRI shows a mass in the right lobe of the liver with mild-moderate hyperintensity on T₂WI (a) and hypointensity on precontrast T₁WI (b). Contrast-enhanced MRI shows typical washin in the arterial phase (c) and washout in the portal venous phase (d). The 3D elastogram (e) shows that the HCC is soft. The mean tumor stiffness was 3.04 kPa and the mean liver parenchyma stiffness was 3.02 kPa. Photomicrograph (f) of H&E-stained ($\times 100$) shows tumor, noncancerous liver tissue, and tumor capsule (black arrow).

Patient Demographic Data and Comparison of Patient Characteristics According to Recurrence

TABLE 1.

Characteristics	Patients (N = 99)	No recurrence (N = 70)	Recurrence (N = 29)	P value
Demographics				
Age, y	49.79 ± 11.39	50.23 ± 11.26	48.72 ± 11.83	0.553
Male sex ^b	90 (91%)	64 (91%)	26 (90%)	1
BMI, kg/m ²	22.02 (19.92–24.91)	22.54 (20.31–24.95)	21.48 (19.51–24.15)	0.329
Biochemical profile				
ALT Level, ^a IU/L	23.00 (33.00–46.00)	32.00 (23.00–46.75)	35.00 (23.50–48.00)	0.503
AST Level, ^a IU/L	33.00 (26.00–44.00)	31.00 (25.00–44.00)	40.00 (30.50–62.00)	0.034
AST/ALT ^a	1.09 (0.84–1.32)	0.99 (0.83–1.25)	1.27 (0.97–1.46)	0.014
TBL, ^a mg/dL	12.80 (10.00–17.00)	12.50 (9.83–16.93)	12.90 (10.10–18.10)	0.628
HBVDNA, ^a × 10 ⁵ IU/ml	0.02 (0.0001–1.14)	0.004 (0.0001–0.60)	0.43 (0.005–4.50)	0.010
PT, ^a sec	13.70 (13.30–14.20)	13.70 (13.34–14.13)	13.70 (13.20–14.30)	0.960
AFP, ^a ng/ml	19.10 (5.98–365.45)	16.78 (5.20–260.35)	94.55 (9.71–669.55)	0.136
Hemoglobin, ^a g/L	139.77 ± 20.12	139.84 ± 21.00	139.59 ± 18.15	0.954
WBC, ^a × 10 ⁹ /L	6.35 (5.50–7.63)	6.38 (5.51–7.67)	6.35 (5.38–7.39)	0.546
Sodium, ^a mmol/L	141.00 (140.00–143.00)	141.00 (139.00–143.00)	141.00 (140.00–142.00)	0.324
Creatinine, ^a umol/L	79.94 ± 13.16	79.12 ± 12.99	81.91 ± 13.60	0.340
NLR ^a	2.10 (1.48–2.88)	2.12 (1.45–2.83)	2.09 (1.50–3.24)	0.623
Platelet, ^a × 10 ⁹ /L	182.00 (134.50–243.25)	177.00 (131.50–238.00)	194.00 (143.50–252.00)	0.373
Albumin, ^a g/L	41.51 ± 4.19	41.73 ± 3.84	40.97 ± 4.95	0.410
Radiological characteristics Tumor stiffness, ^a kPa	5.26 (4.20–6.85)	4.87 (4.08–6.57)	5.89 (4.34–9.10)	0.031
Tumor number ^b				0.300

Characteristics	Patients (N = 99)	No recurrence (N = 70)	Recurrence (N = 29)	P value
Single	72 (73%)	53 (76%)	19 (66%)	
Multiple	27 (27%)	17 (24%)	10 (34%)	
Tumor size, ^a mm	48.00 (37.00–72.00)	46.00 (36.00–65.50)	61.00 (43.50–84.00)	0.015
Tumor size group ^b				0.009
<50 mm	51 (52%)	42 (60%)	9 (31%)	
50 mm	48 (48%)	28 (40%)	20 (69%)	
Classification system (T stage) ^b				0.007
Early (I & II)	73 (74%)	57 (81%)	16 (55%)	
Advanced (III & IV)	26 (26%)	13 (19%)	13 (45%)	
Histological characteristics				
Differentiation ^b				0.056
Well+moderate	84 (85%)	63 (90%)	21 (72%)	
Poor	15 (15%)	7 (10%)	8 (28%)	
Capsule ^b				<0.001
Absent	27 (27%)	12 (17%)	15 (52%)	
Present	72 (73%)	58 (83%)	14 (48%)	
Vascular invasion ^b				0.010
Absent	40 (40%)	34 (49%)	6 (21%)	
Present	59 (60%)	36 (51%)	23 (79%)	
Fibrosis stage ^b				0.324
Early (F0–F2)	37 (37%)	24 (34%)	13 (45%)	
Advanced (F3–F4)	62 (63%)	46 (66%)	16 (55%)	
Child-Pugh class ^b				0.972
Class A	94 (95%)	67 (96%)	27 (93%)	
Class B	5 (5%)	3 (4%)	2 (7%)	
MELD score ^a	4.58 ± 2.69	4.45 ± 2.61	4.88 ± 2.91	0.466

Author Manuscript

Author Manuscript

Author Manuscript

Author Manuscript

BMI: body mass index; AST: aspartate aminotransferase; ALT: alanine aminotransferase; TBIL: total bilirubin; PT: prothrombin time; WBC: white blood cell; NLR: neutrophil-to-lymphocyte ratio; MELD: Model for Endstage Liver Disease score.

^aData are continuous variables, reported as mean \pm standard deviation (SD) or median (interquartile range, IQR), and were compared using the two-sample *t*-test or nonparametric Mann–Whitney test.

^bData are categorical variables, presented as numbers of patients, with percentages in parentheses, and were compared using the chi-square test or Fisher’s exact test.

Univariate and Multivariate Risk Factors Associated With HCC Recurrence After Hepatectomy

TABLE 2.

Variable	Univariate analysis			Multivariate analysis		
	HR	95% CI	P value	HR	95% CI	P value
Age	0.992	0.958–1.027	0.646			
Gender (male)	1.122	0.337–3.733	0.852			
AST/ALT	1.417	0.789–2.545	0.243			
AST level, IU/L	1.004	0.995–1.012	0.418			
AFP, × 10 ³ ng/ml	0.998	0.979–1.018	0.867			
HBV-DNA, × 10 ⁵ IU/ml	0.999	0.997–1.001	0.415			
BMI, kg/m ²	0.963	0.892–1.040	0.335			
Number	1.586	0.730–3.447	0.244			
Size	2.618	1.190–5.758	0.017			
Histological grade	2.527	1.093–5.843	0.030			
Vascular invasion	3.695	1.402–9.736	0.008	2.922	1.079–7.914	0.035
Capsule	3.087	1.479–6.442	0.003			
Liver parenchyma stiffness, kPa	0.931	0.679–1.276	0.699			
Fibrosis stage	0.749	0.360–1.560	0.440			
Stiffness (continuous variable)	1.203	1.095–1.321	<0.001	1.163	1.055–1.282	0.002

Univariate and Multivariate Risk Factors Associated With HCC Recurrence After Hepatectomy (72 single HCCs)

TABLE 3.

Variable	Univariate analysis			Multivariate analysis		
	HR	95% CI	P value	HR	95% CI	P value
Age	0.981	0.939–1.025	0.393			
Gender (male)	0.873	0.249–3.063	0.832			
AST/ALT	1.494	0.757–2.950	0.247			
AST level, IU/L	1.006	0.997–1.015	0.176			
AFP × 10 ³ ng/ml	1.281	0.501–3.276	0.605			
HBV-DNA, × 10 ⁵ IU/ml	0.927	0.212–4.059	0.920			
BMI, kg/m ²	0.952	0.851–1.065	0.387			
Size	3.131	1.184–8.282	0.021			
Histological grade	1.934	0.673–5.556	0.220			
Vascular invasion	4.434	1.289–15.251	0.018	3.773	1.073–13.264	0.038
Capsule	3.713	1.430–9.640	0.007			
Liver parenchyma stiffness, kPa	1.149	0.828–1.594	0.406			
Fibrosis stage	0.763	0.288–2.024	0.587			
Tumor stiffness	1.196	1.055–1.356	0.005	1.150	1.013–1.307	0.031